June 5, 2000

X-ray rocking curve analysis of tetragonally distorted ternary semiconductors on mismatched (001) substrates

X. G. Zhang, *University of Connecticut*
David W Parent, *University of Connecticut*
P. Li, *University of Connecticut*
A. Rodriguez, *University of Connecticut*
G. Zhao, *University of Connecticut*, et al.

X-ray rocking curve analysis of tetragonally distorted ternary semiconductors on mismatched (001) substrates

X. G. Zhang, D. W. Parent, P. Li, A. Rodriguez, G. Zhao, J. E. Ayers,[a] and F. C. Jain
Electrical and Computer Engineering Department, University of Connecticut, Storrs, Connecticut 06269-2157

(Received 30 July 1999; accepted 28 February 2000)

For ternary heteroepitaxial layers, the independent determination of the composition and state of strain requires x-ray rocking curve measurements for at least two different *hkl* reflections because the relaxed lattice constant is a function of the composition. The usual approach involves the use of one symmetric reflection and one asymmetric reflection. Two rocking curves are measured at opposing azimuths for each *hkl* reflection. Thus, it is possible to account for tilting of the *hkl* planes in the epitaxial layer with respect to the *hkl* planes in the substrate, by averaging the peak separations obtained at the opposing azimuths. This procedure presents a practical problem in the case of asymmetric reflections, for which the tilting can only be canceled if the rocking curve for one azimuth is obtained using $\theta-\phi$ incidence. A preferable approach, which provides sharper, more intense rocking curves and greater experimental accuracy, is to measure both asymmetric rocking curves at $\theta+\phi$ incidence. This approach requires that the data be corrected for the tilting of the asymmetric planes introduced by tetragonal distortion. Here we have presented a new analytic procedure that incorporates the tilting of asymmetric diffracting planes due to tetragonal distortion. The new procedure allows the measurement of all rocking curves at $\theta+\phi$ incidence. We have applied this new method to the case of ZnS_ySe_{1-y} grown heteroepitaxially on GaAs (001), using 004 and 044 x-ray rocking curves. We have shown that neglect of the tilting in asymmetric planes results in gross errors in the calculated values of composition (as much as 35 times) and in-plane strain (as much as 2.6 times) for this material.
[S0734-211X(00)06403-9]

I. INTRODUCTION

Ternary and quaternary alloys of zincblende semiconductors are important for the fabrication of high-performance transistors, such as heterojunction bipolar transistors and high electron mobility field effect transistors, as well as optoelectronic devices, including laser diodes, modulators, and detectors. The composition and state of strain in an alloy semiconductor greatly affect device performance. Therefore, much effort has been devoted to the characterization of these materials by x-ray diffraction and photoluminescence.

In the case of a ternary heteroepitaxial layer, the independent determination of the relaxed lattice constant (and therefore the composition) and state of strain requires at least two x-ray rocking curve measurements. This is because the relaxed lattice constant is a function of the composition. Sometimes the analysis is simplified with the assumption that the heteroepitaxial layer has grown coherently on the substrate.[1–3] With this ''pseudomorphic''assumption, the in-plane lattice constant is assumed to be equal to the substrate lattice constant. Then a single rocking curve measurement, using a symmetric reflection, is sufficient for the estimation of the composition and state of strain in a ternary layer. This simplified approach has been extended to quaternary semiconductors, for which a single x-ray measurement is combined with a photoluminescence measurement to determine the relaxed lattice constant and band gap for the material. Such a simplified approach is suitable for a heteroepitaxial system such as AlGaAs/GaAs, for which the lattice mismatch is small over the entire range of aluminum composition. In other heteroepitaxial systems, the possibility of partial lattice relaxation mandates the use of at least two different x-ray rocking curve measurements.

Typically, for heteroepitaxy on a (001) substrate, rocking curves are obtained for one symmetric reflection such as the 004 and one asymmetric reflection such as the 115 or 044. Then, with the assumption that the strained alloy layer is distorted tetragonally, the in-plane and out-of-plane lattice constants (a and c, respectively) may be determined. A complication that arises in this procedure is the tilting of the asymmetric diffracting planes, which is caused by the tetragonal distortion.

In this article, we describe a procedure for the determination of a self-consistent set of values for the in-plane lattice constant, the out-of-plane lattice constant, and the tilting of the asymmetric diffracting planes, using measurements of asymmetric rocking curves with only $\theta+\phi$ incidence. We have also demonstrated the procedure by applying it to the case of heteroepitaxial ZnS_ySe_{1-y} grown on GaAs (001) substrates, using 004 and 044 x-ray rocking curves. We show that gross errors result if the composition and strain in the ternary layer are calculated by neglecting the tilting of the 044 planes due to tetragonal distortion.

[a]Author to whom all correspondence should be addressed; present address: University of Connecticut, 260 Glenbrook Road, Storrs, CT 06269-2157; electronic mail: jayers@engr.uconn.edu

II. THEORY

When using symmetric x-ray rocking curves for heteroepitaxial layers [for example, the 004 reflection for the (001) heteroepitaxial samples] it is necessary to measure the peak separation $\Delta\theta$ at a minimum of two azimuths in order to determine the difference in Bragg angles $\Delta\theta_B$.[4] This is because there is, in general, a tilting of the heteroepitaxial layer with respect to the substrate.[5–12] Thus, the [001] axes of the two are not parallel. The rocking curve peak separation is then[13]

$$\Delta\theta=\Delta\theta_B+\Delta\phi_0\cos(\omega-\omega_0), \tag{1}$$

where $\Delta\theta$ is the rocking curve peak separation measured at an azimuth ω, $\Delta\theta_B$ is the Bragg angle difference between the heteroepitaxial layer and the substrate, $\Delta\phi_0$ is the tilt between the [001] axes of the substrate and the epitaxial layer, and ω_0 specifies the direction of the tilt. Thus, the effect of $\Delta\phi_0$ on the measured peak separations can be eliminated by recording the rocking curves at opposing azimuths (i.e., $\omega=0°$ and $\omega=180°$).

An additional complication arises if one attempts to use the above approach with an asymmetric reflection [for example, the 044 reflection for (001) heteroepitaxial samples]. In such cases there is an additional tilt component $\Delta\phi_{\text{tet}}$ if the heteroepitaxial layer is tetragonally distorted:

$$\Delta\theta=\Delta\theta_B+\Delta\phi_0\cos(\omega-\omega_0)+\Delta\phi_{\text{tet}}. \tag{2}$$

As before, the measurement of the asymmetric rocking curves at opposing azimuths, *for the same set of planes,* allows elimination of the tilt component $\Delta\phi_{\text{tet}}$. That approach has been described in detail previously.[14–16] However, the disadvantage of that approach is that it requires measuring the rocking curve for one azimuth using $\theta-\phi$ incidence. This leads to a relatively weak rocking curve peak and requires longer scanning time compared to using $\theta+\phi$ incidence (Fig. 1 shows the $\theta+\phi$ and $\theta-\phi$ geometries as used in this approach). The reflected intensity ratio for the two geometries can be estimated as[17]

$$\frac{I(\theta+\phi)}{I(\theta-\phi)}=\frac{\sin^2(\theta+\phi)}{\sin^2(\theta-\phi)}, \tag{3}$$

where $I(\theta+\phi)$ and $I(\theta-\phi)$ are the reflected intensities for the cases of $\theta+\phi$ and $\theta-\phi$ incidence, respectively. For example, in the case of the 044 reflection from (001) GaAs, the ratio is 112. This means that the reflected intensity for the $\theta-\phi$ incidence may be insufficient for the purpose of an accurate measurement in that case. Thus, it is generally desirable to measure both asymmetric rocking curves (at the two opposing azimuths) with only $\theta+\phi$ incidence (as shown in Fig. 2), to obtain rocking curve peaks with optimum intensity and full width at half maximum. This minimizes the experimental uncertainty in the measured peak separation. However, $\Delta\phi_{\text{tet}}$ has the same sign for both measurements and cannot be eliminated by taking the average value of the peak separation as before. Nonetheless, $\Delta\phi_{\text{tet}}$ can be calculated from knowledge of the strained lattice constants in the heteroepitaxial layer. For the common case of (001) heteroepitaxy, strain in the grown layer results in tetragonal distortion. Then for the *hkl* reflection, $\Delta\phi_{\text{tet}}$ is given by

$$\Delta\phi_{\text{tet}}=\cos^{-1}\left(\frac{l/c}{\sqrt{(h/a)^2+(k/a)^2+(l/c)^2}}\right)-\cos^{-1}\left(\frac{1}{\sqrt{h^2+k^2+l^2}}\right), \tag{4}$$

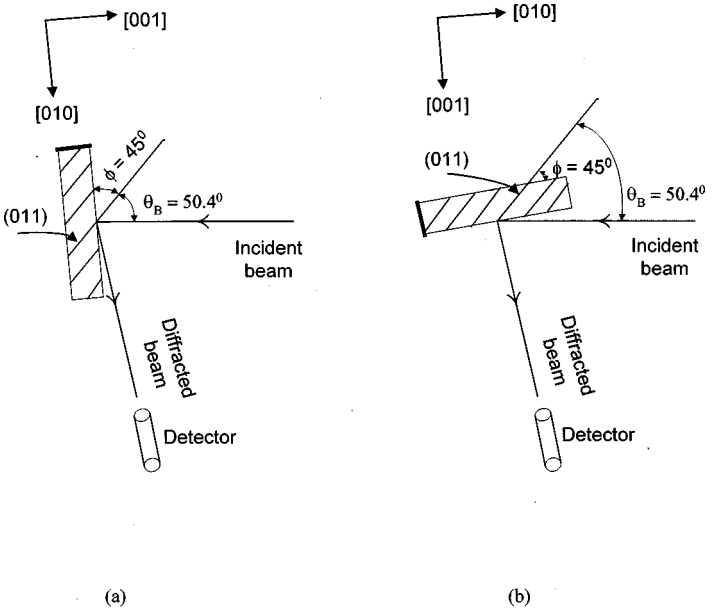

FIG. 1. Asymmetric 044 reflections at opposing azimuths using the same set of diffraction planes. (a) $\omega=0°$ with $\theta+\phi$ incidence and (b) $\omega=180°$ with $\theta-\phi$ incidence. The ω axis is parallel to the [001] direction and perpendicular to the sample surface. The $\omega=180°$ rocking curve must be obtained with the $\theta-\phi$ incidence in this case.

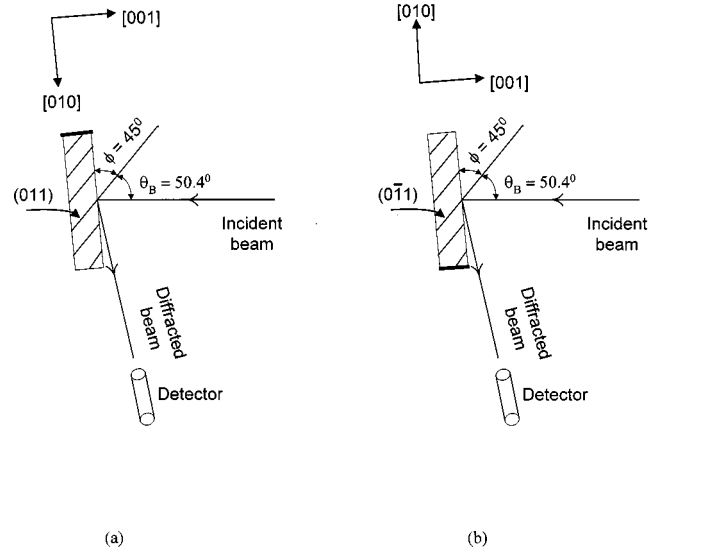

FIG. 2. Asymmetric 044 reflection at opposing azimuths using two different sets of planes. (a) $\omega=0°$ and (b) $\omega=180°$. Both rocking curves may be obtained with the $\theta+\phi$ incidence in this case.

where a and c are the in-plane and out-of plane lattice constants for the heteroepitaxial layer, respectively, and the substrate has been assumed to be unstrained. Thus, for measurements with $\theta+\phi$ incidence, biaxial compression causes $\Delta\phi_{\text{tet}}$ to be positive while biaxial tension causes $\Delta\phi_{\text{tet}}$ to be negative.

For the rocking curve analysis of a ternary heteroepitaxial layer on a (001) substrate, the ideal procedure is as follows: First, a symmetric 00m reflection is measured at two opposing azimuths and the out-of-plane lattice constant is determined from the average peak separation $\Delta\theta_{\text{ave}}$. Using the 00$m$ reflection,

$$c=\frac{m\lambda}{2\sin(\theta_{B00m,\text{substrate}}+\Delta\theta_{\text{ave},00m})}, \tag{5}$$

where λ is the x-ray wavelength. Next, an asymmetric hkl reflection is measured with $\theta+\phi$ incidence at two opposing azimuths. The spacing for the hkl planes can be determined as

$$d_{hkl}=\frac{\lambda}{2\sin(\theta_{Bhkl,\text{substrate}}+\Delta\theta_{\text{ave},hkl}-\Delta\phi_{\text{tet}})}, \tag{6}$$

where $\Delta\theta_{\text{ave},hkl}$ is the average peak separation for the hkl reflection. Then the in-plane lattice constant may be determined from

$$a=\left(\frac{h^2+k^2}{l^2/c^2-1/d_{hkl}^2}\right)^{-1/2}. \tag{7}$$

If Eqs. (6), (7), and (4) are solved iteratively, starting with any particular value of $\Delta\phi_{\text{tet}}$, then the end result will be a consistent set of values for c, a, and $\Delta\phi_{\text{tet}}$. Then the relaxed lattice constant a_0 and state of strain ϵ may be determined for the heteroepitaxial layer using

$$a_0=\frac{c+\left(\frac{2\nu}{1-\nu}\right)a}{1+\left(\frac{2\nu}{1-\nu}\right)}, \tag{8}$$

$$\varepsilon_{\text{in-plane}}=\frac{a-a_0}{a_0}, \tag{9}$$

and

$$\varepsilon_{\text{out-of-plane}}=\frac{c-a_0}{a_0}, \tag{10}$$

where ν is the Poisson ratio of the heteroepitaxial layer which is defined as the negative of the ratio between lateral and longitudinal strains under uniaxial longitudinal stress and is related to the elastic stiffness constants C_{11} and C_{12} as

$$\nu[001]=\frac{C_{12}}{(C_{11}+C_{12})} \tag{11}$$

for the [001] orientation.

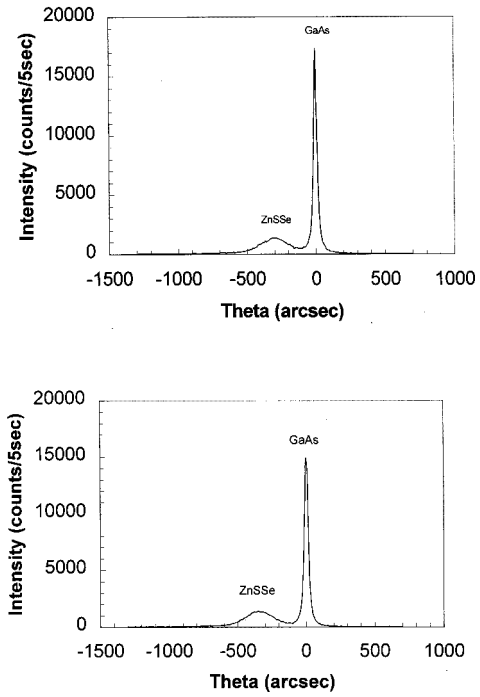

FIG. 3. 004 rocking curves for sample 744. Top: The azimuth was 180°. Bottom: the azimuth was 0°.

III. EXPERIMENT

For this study, ZnS_ySe_{1-y} heterostructures were grown on semi-insulating GaAs (001) $\pm 0.5°$ substrates supplied by Atomergic Chemetals. Prior to epitaxy, the substrates were cleaned sequentially in boiling trichloroethylene, acetone, and methanol. After rinsing in deionized water, the substrates were etched for 3 min in Caro's etch of a 5:1:1 H_2SO_4:H_2O_2:H_2O composition, at a temperature of 60 °C. After a second rinse in deionized water, the substrates were treated for one minute in 1:1 HC1:H_2O to remove the native oxide. Finally, substrates were rinsed in deionized water, then boiling isopropanol, and loaded into the reaction chamber.

A vertical, stainless steel EMCORE reactor with a rotating, resistively heated molybdenum susceptor was used. All growth runs were carried out at 250 Torr with 350 rpm susceptor rotation, and with 14.25 slm of palladium-diffused hydrogen as the carrier gas. The photoirradiation was achieved using an Oriel Hg arc lamp operated at 150 W electrical power. The ultraviolet (UV) irradiation was brought into the reaction chamber using a mirror and a quartz window, resulting in normal incidence on the sample. Neutral density filters were used to adjust the irradiation intensity. All irradiation intensities reported were measured using an intensity meter (manufactured by HTG) outside of the reaction chamber.

Prior to growth, the substrates were held at 610 °C for 2 min in pure hydrogen to remove oxygen and carbon contamination. Growth was always initiated or restarted on Se-stabilized surfaces (the DMSe flow was started 1 min before the DMZn flow). The growth was interrupted for tem-

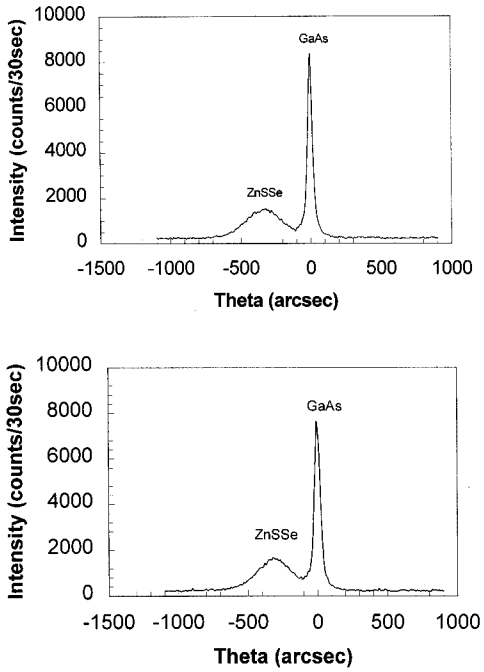

FIG. 4. 044 rocking curves for sample 744 both at $\theta+\phi$ incidence. Top: the azimuth was 45°. Bottom: The azimuth was 225°.

perature ramps and changes in ultraviolet intensity.

A high-temperature ZnSe buffer layer was always grown first, at 595 °C and without UV irritation, because photoassisted metalorganic vapor phase epitaxy growth cannot be initiated directly on the bare GaAs surface. The reactant mole fractions were 10^{-4} (DMZn) and 2×10^{-4} (DMSe) for the high-temperature buffer. The total thickness of the two ZnSe buffer layers was 130 nm.

ZnS_ySe_{1-y} was grown on top of the ZnSe buffer layers at 360 °C and with the incident irradiation intensity adjusted to 36 m W/cm^2, with a growth time of 45 min. The reactant mole fractions were 10^{-4} (DMZn), 2×10^{-4} (DMSe) and 0 to 2.5×10^{-4} (DES).

The heteroepitaxial samples were characterized by high-resolution x-ray diffraction using a Bartels five-crystal x-ray diffractometer described previously.[18,19] The Philips fixed-anode Cu x-ray source was operated at 40 kV and 20 mA. The line-focused beam was slit limited to 5 mm length normal to the plane of the diffractometer and 0.5 mm width in the plane of the diffractometer by pairs of slits placed on either side of the monochromator. The spacing between the slits was 210 mm. A four-crystal Bartels-type monochromator was employed using four Ge 022 reflections from Ge (011) crystals arranged in the (+, −, −, +) geometry and tuned to the Cu $K\alpha_1$ lined ($\lambda=1.540\,594$ Å). 004 and 044 rocking curves were measured at 293 K using the (+, −, −, +, −) and (+, −, −, +, +) geometry. For each rocking curve measurement, the specimen tilt was adjusted to bring the specimen diffraction vector into the plane of the diffractometer. Tilt optimization was performed by adjusting the tilt for maximum peak reflected intensity and with a precision of $\pm0.5°$.

TABLE I. Summary of measured 004 and 044 rocking curve data for the different samples investigated. $\Delta\theta$ is the peak separation between the ZnS_ySe_{1-y} and the GaAs. ω is the azimuth.

Sample	$\Delta\theta_{004}$ (arc sec) ($\omega=0°$)	$\Delta\theta_{004}$ (arc sec) ($\omega=180°$)	$\Delta\theta_{044}$ (arc sec) ($\omega=45°$)	$\Delta\theta_{044}$ (arc sec) ($\omega=225°$)
743	−441	−425	−420	−340
744	−350	−325	−320	−320
745	−180	−190	−90	−90
751	−90	−70	−90	−120
746	110	125	−130	−120
748	340	340	−120	−90
749	570	520	150	120

TABLE II. Summary of the calculated results for the different samples investigated. c, a, and a_0 are the out-of-plane, the in-plane and the relaxed lattice constants of the ZnS_ySe_{1-y} epitaxial layer, respectively. y is the solid phase composition. a, a_0, and y have been calculated by correcting the tilting of the 044 planes, $\Delta\phi_{tet}$.

Sample	c (Å)	a (Å)	a_0 (Å)	y (%)
743	5.6716	5.6660	5.6685	0.08
744	5.6677	5.6600	5.6635	2.0
745	5.6611	5.6547	5.6576	4.3
751	5.6567	5.6556	5.6561	4.9
746	5.6483	5.6571	5.6531	6.04
748	5.6391	5.6573	5.6490	7.6
749	5.6305	5.6526	5.6426	10.1

Two symmetric 004 reflections and two asymmetric 044 reflections have been measured at two opposing azimuths from each sample. Figure 3 shows the 004 rocking curves for sample 744 for $\omega=0°$, 180°, ω being the azimuth. Two diffraction peaks are observed, one for the GaAs and one for the ZnS_ySe_{1-y}. The peak of the pseudomorphic ZnSe buffer layer, which is observed from other samples, is merged in the left tail of the ZnS_ySe_{1-y} peak. Typical intensities measured with a Bicron scintillation counter were 3000 counts s^{-1} for the GaAs 004, 300 counts s^{-1} for the ZnSe 004, and 1500 counts s^{-1} for the ZnS_ySe_{1-y} 004. The measured 004 rocking curve peak separation between the GaAs and the ZnSe is about 780 arc sec for the analyzed samples. Figure 4 shows the 044 rocking curves for sample 744 for $\omega=45°$ and 225° both at $\theta+\phi$ incidence. While there was sufficient x-ray intensity to clearly resolve the ZnS_ySe_{1-y} peak, the peak of the ZnSe buffer layer was too weak to be resolved.

The summary of measured 004 and 044 rocking curve data and the calculated results for all of the analyzed samples is reported in Tables I and II, respectively. To determine the peak separation accurately, the 004 and 044 rocking curve profiles for the GaAs, ZnSe, and ZnS_ySe_{1-y} were extracted by least squares fitting to Lorentzian profiles (GaAs) and Gaussian profiles (ZnSe and ZnS_ySe_{1-y}). The peak separations could be evaluated with an accuracy of ±1.5 arc sec. The procedure for the determination of a self-consistent set of values for the out-of-plane lattice constant c, the in-plane lattice constant a, and the relaxed lattice constant a_0 for the ZnS_ySe_{1-y} epitaxial layers are as the follows: (1) Determine the out-of-plane lattice constant from the 004 measurement.

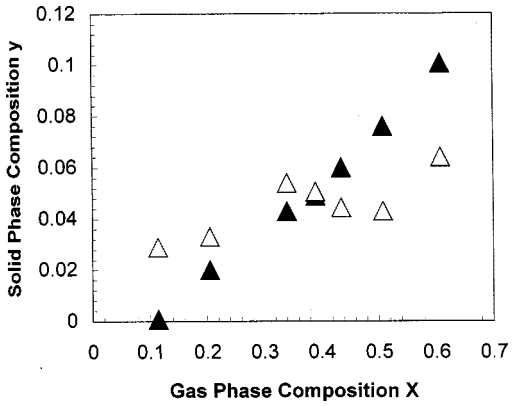

FIG. 5. Solid phase composition y in ZnS_ySe_{1-y} vs the gas phase composition X ($X=X_{DES}/(X_{DES}+X_{DMSe})$) for growth at 360 °C with an irradiation intensity of 36 mW/cm^2. The filled triangles represent data corrected for the tilting of the 044 planes, $\Delta\phi_{tet}$; unfilled triangles represent uncorrected data.

(2) Determine the in-plane lattice constant from the 004 and the 044 measurements. In this step, iteration is involved to obtain an accurate value of the in-plane lattice constant by correcting for the tilting of the 044 planes, $\Delta\phi_{tet}$. (3) Determine the relaxed lattice constant from the out-of-plane and the in-plane lattice constants using Eq. (8) with a Poisson ratio of $\nu=0.375$. Then, from the lattice constants of $a_{ZnSe}=5.6687$ Å, $a_{ZnS}=5.4105$ Å, and the obtained relaxed lattice constant a_0, the solid composition y for the ZnS_ySe_{1-y} epitaxial layers can be calculated according to Vegard's law. Here a ZnSe Poisson ratio of $\nu_{ZnSe}=0.375$ was used, instead of the corresponding value for ZnS_ySe_{1-y}, which may be determined according to Vegard's law. This approach greatly reduces the amount of calculations without a loss of accuracy, since the Poisson ratio in zincblende (β-phase) ZnS, with a value of $\nu_{\beta\text{-ZnS}}=0.325$, is close to that of ZnSe.

IV. RESULTS AND DISCUSSION FOR ZnS_ySe_{1-y} GROWN ON GAAS (001)

Figure 5 shows the solid phase composition y versus the gas phase composition X, for ZnS_ySe_{1-y} grown at 360 °C with 36 mW/cm^2 photoirradiation. The filled triangles represent data corrected for the tilting of the asymmetric planes while the unfilled triangles represent uncorrected data. It can be seen that gross errors (as much as 35 times) result in the calculated value of solid composition if $\Delta\phi_{tet}$ is neglected. Neglect of $\Delta\phi_{tet}$ results in overestimation of y for $y<0.05$, and underestimation for y for $y>0.05$ in this case. Because of this, the gross errors associated with neglecting $\Delta\phi_{tet}$ make the compositional characteristic appear nonmonotonic.

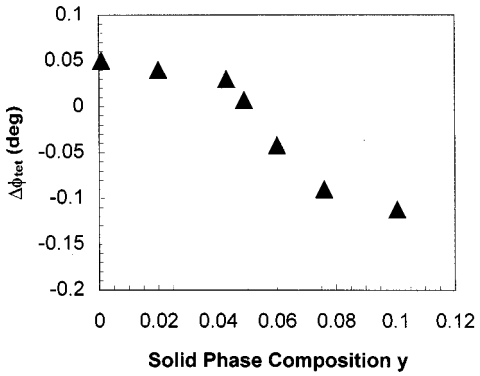

FIG. 7. $\Delta\phi_{tet}$ vs the solid composition y, for ZnS_ySe_{1-y} grown on GaAs (001) at 360 °C with an intermediate 130 nm ZnSe buffer.

Figure 6 shows the in-plane strain versus the solid composition y, for the same set of ZnS_ySe_{1-y} samples. The filled triangles represent data corrected for the tilting of the asymmetric planes while the unfilled triangles represent uncorrected data. Here, too, neglect of $\Delta\phi_{tet}$ results in gross errors (as much as 2.6 times). The absolute value of in-plane strain is overestimated if $\Delta\phi_{tet}$ is neglected, except for in the vicinity of $y\approx0.05$.

Figure 7 shows the tilting of the (044) planes due to the tetragonal distortion, versus the solid composition y. $\Delta\phi_{tet}$ ranges from $-0.112°$ to $+0.052°$ (-403 to $+187$ arc sec). Clearly, such large tilt contributions must be accounted for to avoid large errors in the analysis.

Figure 8 shows the error in the calculated composition y versus $\Delta\phi_{tet}$ for the case in which $\Delta\phi_{tet}$ is neglected. The

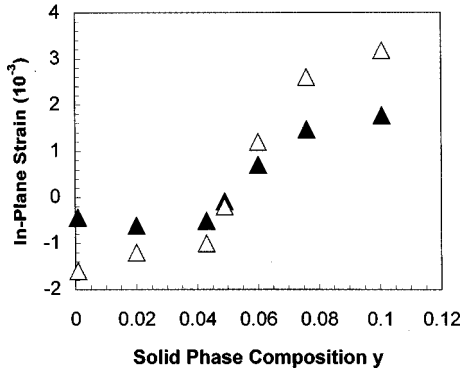

FIG. 6. In-plane strain vs the solid composition y, for ZnS_ySe_{1-y} grown on GaAs (001) at 360 °C with an intermediate 130 nm ZnSe buffer. The filled triangles represent data corrected for the tilting of the 044 planes, $\Delta\phi_{tet}$; unfilled triangles represent uncorrected data.

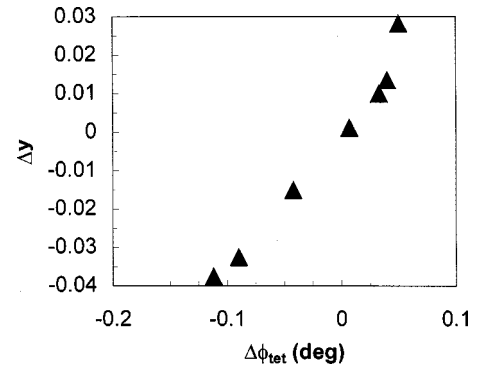

FIG. 8. Δy vs $\Delta\phi_{tet}$. Δy is the error in the calculated composition if $\Delta\phi_{tet}$ is neglected.

relationship is approximately linear, as expected from the differential form of the Bragg law.

V. CONCLUSION

We have presented a new analytic procedure that incorporates the tilting of asymmetric diffracting planes due to tetragonal distortion. The new procedure allows the measurement of all rocking curves at $\theta+\phi$ incidence. We have applied this new method to the case of ZnS_ySe_{1-y} grown heteroepitaxially on GaAs (001), using 004 and 044 x-ray rocking curves. We have shown that neglect of the tilting in asymmetric planes results in gross errors in the calculated values of composition (as much as 35 times) and in-plane strain (as much as 2.6 times) for this material.

ACKNOWLEDGMENTS

This work was supported by the National Science Foundation, Grant No. ECS-9309079; by the Connecticut Department of Economic Development, Grant Nos. 90-606, 92K-016, and 97G-025. This support is gratefully acknowledged.

[1]E. Estop, A. Izrael, and M. Sauvage, Acta Crystallogr., Sect. A: Cryst. Phys., Diffr., Theor. Gen. Crystallogr. **32**, 627 (1976).
[2]J. Hornstra and W. J. Bartels, J. Cryst. Growth **44**, 521 (1978).
[3]W. J. Bartels and W. Nijman, J. Cryst. Growth **44**, 518 (1978).
[4]J. Matsui, K. Onabe, T. Kamejima, and I. Hayashi, J. Electrochem. Soc. **126**, 664 (1979).
[5]H. Nagai, J. Appl. Phys. **45**, 3789 (1974).
[6]G. H. Olsen and R. T. Smith, Phys. Status Solidi A **31**, 739 (1975).
[7]E. Yamaguchi, I. Takayasu, T. Minato, and M. Kawashima, J. Appl. Phys. **62**, 885 (1987).
[8]J. Kleiman, R. M. Park, and H. A. Mar, J. Appl. Phys. **64**, 1201 (1988).
[9]A. Ohki, N. Shibata, and S. Zenbutsu, J. Appl. Phys. **64**, 694 (1988).
[10]I. B. Bhat, K. Patel, N. R. Taskar, J. E. Ayers, and S. K. Ghandhi, J. Cryst. Growth **88**, 23 (1988).
[11]W. L. Ahlgren *et al.*, J. Vac. Sci. Technol. A **7**, 331 (1989).
[12]J. E. Ayers, S. K. Ghandhi, and L. J. Schowalter, J. Cryst. Growth **113**, 430 (1991).
[13]S. K. Ghandhi and J. E. Ayers, Appl. Phys. Lett. **53**, 1204 (1988).
[14]A. T. Macrander, G. P. Schwartz, and G. J. Gualtieri, J. Appl. Phys. **64**, 6736 (1988).
[15]A. Leiberich and J. Levkoff, J. Vac. Sci. Technol. B **8**, 422 (1990).
[16]A. Krost, G. Bauer, and J. Woitok, in *Optical Characterization of Epitaxial Semiconductor Layers*, edited by G. Bauer and W. Richter (Springer, Berlin, 1996), p. 287.
[17]B. E. Warren, *X-Ray Diffraction* (Addison-Wesley, Reading, MA, 1969), p. 353.
[18]P. D. Healey, K. Bao, M. Gokhale, J. E. Ayers, and F. C. Jain, Acta Crystallogr., Sect. A: Found. Crystallogr. **51**, 489 (1995).
[19]P. D. Healey and J. E. Ayers, Acta Crystallogr., Sect. A: Found. Crystallogr. **52**, 245 (1996).